Sand Transport over an Immobile Gravel Substrate

R. A. Kuhnle, M.ASCE[1]; D. G. Wren, M.ASCE[2]; E. J. Langendoen, M.ASCE[3]; and J. R. Rigby[4]

Abstract: Experiments were conducted in a laboratory flume channel to evaluate the effects of increasing amounts of sand on its transport over and through an immobile coarse gravel bed. Detailed measurements of sand transport rate, bed texture, and bed topography were collected for four different discharges at approximately the same flow depth of 0.2 m for 11 different elevations of sand in the gravel bed. Sand transport was measured using both physical samples and a density cell. For a given flow rate, increases in the elevation of sand relative to gravel resulted in decreases of bed shear stress from 32–44% and increases in sand transport by three orders of magnitude. For the highest two discharges, the sand merged into a small number of long and low bed forms that translated through and over the gravel bed. A collapse of the transport data was accomplished by relating the sand transport rate to the bed shear stress scaled by the cumulative probability distribution function of the gravel surface evaluated at the height of the mean sand bed. **DOI: [10.1061/(ASCE)HY.1943-7900.0000615](https://doi.org/10.1061/(ASCE)HY.1943-7900.0000615)**. © 2013 American Society of Civil Engineers.

CE Database subject headings: Sand (hydraulic); Sediment transport; Gravel.

Author keywords: Sand; Gravel; Sediment transport.

Introduction

The movement of sand through gravel sediment is difficult to predict but an important process to understand. The sediment bed of rivers downstream of dams often becomes armored with gravel and deficient in sand-sized sediment (Hathaway 1948; Vanoni 1975, p. 8). Tributaries downstream of dams, reservoir flushing, dam bypassing, or dam removal can intermittently introduce large amounts of sand to armored gravel bed channels. In each of these situations, the prediction of sand transport and flow stage are complicated by the interaction of the sediment and water with the rough bed. The Colorado River in the Grand Canyon is an example of a system where sand influxes are contributed to a coarse bed by tributaries (Topping et al. 2000).

Understanding and predicting the movement and deposition of sand in coarser armored beds is important for maintaining the aquatic habitat of rivers, such as salmonid fisheries (Lisle and Lewis 1992; Alonso et al. 1996). Exchange of gases through the substrate and successful spawning have been found to depend on the state of the fines in the gravel substrate (Alonso et al. 1996). Many streams in which salmonids spawn have been dammed, often resulting in bimodal sand/gravel size distributions with large differences between the modes (Sambrook Smith 1996). Managing these fisheries requires improved knowledge of sediment transport mechanics in sand–gravel systems. For low bed shear stresses, the

sand portion of the bed material is often entrained before the gravel begins to move (Parker 2008), and there may be a substantial range of flow strengths over which only the sand and fine gravel portions of the bed material are entrained and transported (Parker et al. 1982). The main channel of Goodwin Creek, Mississippi, is an example of a stream in which the sand fraction is entrained and transported before the gravel fractions of the bed material (Kuhnle 1992, 1993).

There have been a number of studies that have investigated the effect of sand on the transport of sand–gravel sediment mixtures (e.g., Iseya and Ikeda 1987; Ferguson et al. 1989; Kleinhans 2002; Curran and Wilcock 2005). It has been shown that the bed material load of streams with sand–gravel beds may be reasonably predicted by using an adjustment factor to predict the critical shear stress for each size fraction relative to the mean fraction and a common transport relation (Wilcock and Crowe 2003; Almedeij et al. 2006). Although these approaches yield reasonable results for transport of generally continuous mixtures of sand and gravel, these techniques tend to break down when the sand is being transported among much larger immobile gravel. This is presumably because the bed shear stress does not properly represent the shear stress acting on the sand surface (Wren et al. 2011). Recent theoretical work on modeling the transport of sand over immobile gravel beds has indicated that the bed elevation distribution function, together with a representative grain size and height of the sand bed, may be used to quantify the transport of sand in simple mixed gravel and sand systems (Pellachini 2011). It was shown by Pellachini (2011) that the bed elevation distribution function may be used to scale the shear stress in the gravel layer of mixed sand and gravel systems. Prediction of sand transport in bed materials with immobile gravel substrates is complicated by the variable degree of exposure of the sand bed and the accompanying interplay between the fluid flow and the areas dominated by either sand or gravel. For some combinations of flow and sediment sizes, the sand in the interstices of the gravel sediment may be shielded from the shear stress of the flowing water. For other cases, local perturbations of the flow caused by the immobile gravel may act to increase the shear stress on the interstitial sand (Grams and Wilcock 2007). These competing effects

[1]National Sedimentation Laboratory, USDA-ARS, P.O. Box 1157, Oxford, MS 38655 (corresponding author). E-mail: roger.kuhnle@ars.usda.gov

[2]National Sedimentation Laboratory, USDA-ARS, P.O. Box 1157, Oxford, MS 38655. E-mail: daniel.wren@ars.usda.gov

[3]National Sedimentation Laboratory, USDA-ARS, P.O. Box 1157, Oxford, MS 38655. E-mail: eddy.langendoen@ars.usda.gov

[4]National Sedimentation Laboratory, USDA-ARS, P.O. Box 1157, Oxford, MS 38655. E-mail: jr.rigby@ars.usda.gov

must be resolved before a reasonable prediction of sand transport can be made for these conditions.

This study is different from many previous studies of sand and gravel transport in that the sand and gravel sediments are separated by a large size range (∼100×). This large size difference dictates that the sand will not form a seal or bridge, but will fill the voids of the gravel from the bottom up (Gibson et al. 2009). Other studies have considered the transport of sand over coarse immobile beds (Grams and Wilcock 2007; Tuijnder 2010; Papanicolaou et al. 2011). The study conducted by Grams and Wilcock (2007) considered the transport of fine sand in suspension over fixed gravel-sized hemispheres, whereas Tuijnder (2010) studied the formation of bed forms and transport of supply-limited coarse sand ($D_{50} = 0.8$ mm) over immobile fine gravel ($D_{50} = 10.9$ mm). Papanicolaou et al. (2011) studied the role of nonmoving clasts with a packing density of 2%, which had a ratio of the flow depth to clast diameter of 0.8, on the movement of coarse sand. Grams and Wilcock (2007) found that the size of the sand, shear stress at the bed, and the elevation of the sand relative to the gravel substrate were the controlling factors necessary to predict the concentration of suspended sand near the gravel bed. Tuijnder (2010) found that the exposure of the immobile layer, the size of the bed forms, and roughness of the bed were needed to predict sand transport rate. Bed load rate was found to be reduced by a factor of 5 to 20 and grain shear stress was found to represent 67% of the total resistance for the experiments with clasts, as compared with ones without clasts by Papanicolaou et al. (2011). In these previous studies, the transport of sand was predominantly as bed load with little or no suspension (Tuijnder 2010; Papanicolaou et al. 2011) or as suspended load with little bed load (Grams and Wilcock 2007). In contrast, the sand transport regimes in this study included both bed load only and combined bed- and suspended-load through a natural gravel sediment.

Recent efforts to better understand the interaction of rough beds with fluid flow have led to the development of combined spatial/temporal averaging techniques that are referred to as double averaging. Data collected in spatially heterogeneous flows may, in addition to more traditional temporal analysis methods, have supplemental volume or area averaging applied to planes parallel to the mean bed (Nikora et al. 2001, 2007a; McLean and Nikora 2006). The development and use of double averaging has led to dividing the flow field over a rough bed into horizontal layers whose flow characteristics are defined by their position relative to the rough bed (Nikora et al. 2007b) and to statistical techniques for describing the bed roughness (Nikora et al. 2001). A function [$A(z)$] may be defined to represent the roughness of the bed as the cumulative probability distribution of the elevation of the gravel on the bed (Nikora et al. 2001). The cumulative probability distribution provides a representation of the solids and void space in the bed surface layer, and it is reasonable to assume that $A(z)$ will be an important variable in the prediction of the shear stress in the top few centimeters of a gravel bed. A recent study (Stoesser 2010) used a cumulative probability distribution of the elevation of the gravel, generated from the mean diameter of the bed material together with forcing terms in the momentum equations within the framework of large eddy simulation, to successfully simulate a series of mean velocity profiles, turbulent intensities, and turbulent shear stress profiles flows. Although this is an important result, and shows promise for the future by being able to predict roughness geometry functions by using the median diameter of the bed, this method has not been shown to be applicable to conditions where bed sediment was in motion and the bed roughness was changing with time.

The focus of this study was on measuring and predicting the transport of sand over a stationary gravel bed in a laboratory flume. A series of experiments were conducted in which the elevation of the sand relative to the gravel in the flume system was increased in a stepwise manner, and the flow parameters and sediment transport rates were measured for each flow and sediment bed condition. The development of a method for predicting the transport of sand through and over an immobile gravel bed is described.

Experimental Methods

All experiments were conducted at the National Sedimentation Laboratory located in Oxford, Mississippi, in a 15-m long, 0.36-m wide, 0.45-m deep flume channel with an adjustable slope in which sediment and water were recirculated. The sand used in all of the experiments ranged in size from 0.1 to 0.5 mm in diameter with a median grain diameter of 0.30 mm, density (ρ_s) of 2.65 g/cm³, and $(D_{84}/D_{16})^{1/2} = 1.35$ (Fig. 1). The gravel substrate, which was not transported in the experiments, consisted of a randomly placed layer beginning 1.2 m downstream of the head box of the channel and continuing for 13.4 m to just upstream of the tail box, with mean and maximum elevations of 17.5 and 21.44 cm above the bottom of the flume channel, respectively. The gravel ranged in diameter from 27 to 52 mm with a median diameter of 35.0 mm, $\rho_s = 2.65$ g/cm³, and $(D_{84}/D_{16})^{1/2} = 1.15$ (Fig. 1). The upstream 1.2 m of the flume channel consisted of a false bottom with a single layer of gravel glued down so as to prevent its entrainment by the high shear stress of the developing boundary layer.

Bed surface topography was measured using close-range terrestrial digital photogrammetry similar to Hardy et al. (2009). Images were taken with a Pentax K10D digital camera with a Pentax P-DA 18–55-mm F3.5-5.6 lens with an image resolution of $3,872 \times 2,592$ pixels. The camera was mounted on a carriage that traversed the top of the flume. Camera calibration was performed on a checkerboard pattern before and after image acquisition following the procedure of Bouguet (2008) to determine the intrinsic camera parameters and lens distortion. To minimize the error in these parameters, the calibration images covered the entire range in angles (0–90°) and azimuths (0–360°). Variations in intrinsic camera and lens distortion parameters were found to be negligible. Adobe Photoshop was used to convert both calibration and bed surface reconstruction images to portable network graphics (PNG)
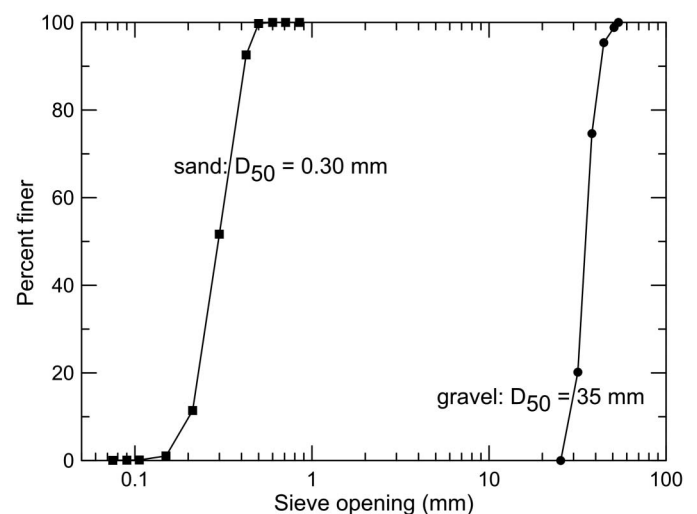

Fig. 1. Grain size distributions of sand and gravel fractions

format, which uses a lossless compression algorithm. Ground control points with an average longitudinal spacing of 5 cm were placed on the gravel surface and their X, Y, and Z coordinates measured using a point gauge with a horizontal and vertical accuracy of 0.5 mm. ERDAS LPS v9.3 (Leica Geosystems 2002) was used to extract a digital elevation model (DEM) of the gravel topography (Lane et al. 2000). The resulting DEMs have a horizontal resolution of 1 mm and a mean vertical root-mean-square (rms) error of approximately 1 mm.

The roughness of the gravel bed was described using the cumulative probability distribution of gravel (CPDG) bed elevations (Fig. 2). This CPDG was calculated using the DEMs derived from digital photogrammetry for a 5-m-long reach of the gravel bed in the channel before sand addition. The 5-m-long reach was centrally located to remove portions of the bed that were influenced by the entrance and exit conditions of the channel. This distribution represents the fraction of the solid material that is located below a particular elevation in the top layer of the bed. For instance, Z_{10} is the elevation for which 10% of the gravel elevations are lower. The values of Z_{50}, Z_{90}, and Z_{100} are defined similarly. There have been several studies that have demonstrated that the distribution of the bed elevations (Fig. 2) is an important variable for predicting flow velocity and shear stress below the Z_{100} level of the bed (e.g., Manes et al. 2007; Aberle et al. 2008; Cooper and Tait 2008; Mignot et al. 2009; Wren et al. 2011).

Flow depth ranged from 0.20 to 0.22 m in the experiments and was measured as the difference between the elevation of the bed and the water surface as determined from stream parallel centerline transects measured over the central 8 m of the channel using acoustic water-surface and bed-surface sensors mounted on a carriage, which rode on rails above the flume channel. Water surface slope was determined as the sum of the slope of the water surface transect relative to the flume rails and the slope of the flume rails. Discharge in the channel was measured using a calibrated Venturi meter read by a pressure transducer in the 0.15-m diameter sediment and water return pipe. Four discharges, nominally 20, 30, 50, and 65 L/s were imposed on each bed mixture of sand and gravel. Shear stress was calculated for each experimental run as

$$\tau = \rho g R S \tag{1}$$

where ρ = density of the water; g = acceleration of gravity; R = hydraulic radius of the flow; and S = slope of the water surface. The boundary shear stress was corrected for the effect of the
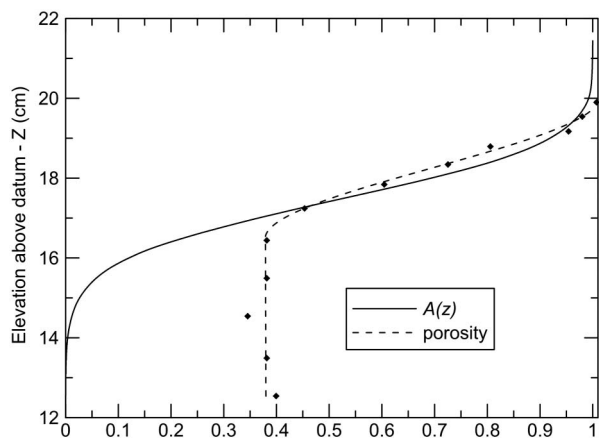
sidewall of the flume using the relation of Vanoni and Brooks (1957). The friction factor of the smooth sidewalls was calculated using Eq. (24) of Chiew and Parker (1994) in place of Fig. 39 of Vanoni and Brooks (1957). The sidewall corrected shear stress will hereafter be termed the bed shear stress (τ_b).

The ratio of the width of the channel in the flume to its depth (aspect ratio) was about 1.7 for all of the experiments in this study. With an aspect ratio of the flow less than 2, there was a concern about the effect of secondary currents, which are generally not important in field channels with larger aspect ratios, on sediment transport. Secondary currents were measured in this flume for a flow depth of 0.18 m, depth-averaged velocity of 0.29 m/s, and with a smooth bottom (Horton 2001). The lateral velocities did not exceed 5.2% of the downstream value. Also, Wren et al. (2011) determined that Reynolds stress profiles extrapolated upward attained a value of zero before reaching the water surface. However, this should have a minimal effect on the present study, since sand-sized sediment is entrained and is predominantly transported in the lowest third of the flow depth (Vanoni 1975).

Sediment transport was measured using a 1.3-cm (1/2-in.) inside diameter sampling nozzle mounted in the center of the return pipe just downstream of the pump impellor. The flow velocity into the sampling nozzle was adjusted to match the mean velocity of the flow in the return pipe (isokinetic) to avoid biasing the concentration of the sediment in the sample. The discharge in the 1.3-cm-diameter sampling line was measured by collecting the flow in a 20-L vessel over a measured period of time and determining the mass of the water on an electronic balance. Total sediment transport rate was determined using two methods, depending on the magnitude of the transport rate in the experiment. The first method, used for low sediment-transport rates, consisted of catching all sand passing through the sampling nozzle using a 0.053-mm sieve that was placed in the stream of water from the sampling line. For higher sediment-transport rates, sediment transport in the sampling line was measured by recording the output from a density cell (Dynatrol model CL-10 HYS) at 0.25 Hz. The density cell consisted of a vibrating u-shaped tube and was calibrated for sediment concentration and flow rate with the same sand used in the experiments. The range of the calibration conditions included the flows and concentrations observed in this study. The mean sediment concentration from the physical samples or from the density cell, which were collected for at least 4 h, were multiplied by the mean flow rate from the Venturi meter to obtain the total sand transport rate (mass/time). For the initial sand elevations ($Z_{01}-Z_{16}$), nearly all of the transport data were collected using a sieve at the end of the sampling line. As sand elevations became greater, sediment concentrations were high enough that the density cell was used to collect sediment transport data for all of the discharges.

Sand was added to the channel near the downstream end over several hours using a vibrating sediment feeder. Only preliminary flow and gravel sediment measurements were conducted on the gravel bed before sand was added to the flume channel. The first sand addition (300 kg) resulted in an elevation of about 5 cm (Z_{01}) below the top of the gravel bed (Fig. 3). Next, the flume was run for approximately 14 h at a discharge of 65 L/s to insure that the elevation of the sand had come to an equilibrium level over the length of the flume and flow was uniform. The attainment of equilibrium in the channel was determined by checking for steady water surface slopes with time. Flume slope was adjusted as necessary after each sand addition and for each flow rate to allow the achievement of equilibrium conditions in the channel. Flow and sediment transport measurements were then collected at four discharges for each bed.

Fig. 2. Cumulative distribution of gravel elevations [$A(z)$] and porosity in the bed surface; the datum is the bottom of the flume channel

Fig. 3. Photographs of sand fill process: (a) side view of filling bed at low discharge; (b) top view of filling at low discharge; (c) side view of filling at high discharge; (d) side view of filling at high discharge at a later time
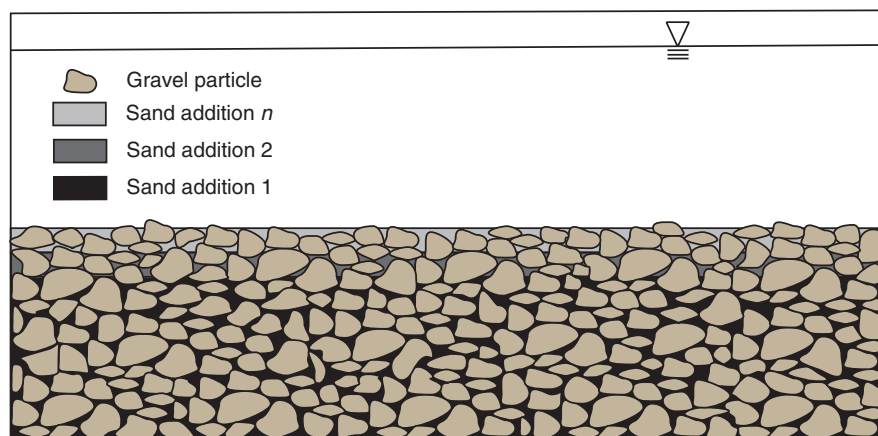

Fig. 4. Schematic sketch of gravel bed being filled with sand

Following the completion of flow and sediment transport measurements for the sand bed at the Z_{01} level, sand was added using the vibrating feeder (Fig. 4), and the flume was run for 14 h at 65 L/s to establish steady uniform-flow conditions in the channel before flow and sediment transport rates were measured at the other discharges. This procedure was repeated for 11 different sand bed elevations from Z_{01} to Z_{98} (Table 1).

The elevation of the sand was measured at 51 points using a point gauge over an 8-m length of the channel. The measurement locations were approximately every 50 cm in the streamwise direction and randomly selected in the cross-stream direction. The sand levels for successive sand additions were calculated using the porosity of the gravel and sand and the dimensions of the gravel bed in the flume. The volume of sand was based on additions of known mass with a measured porosity of 0.4. The increasing porosity of the top layer of gravel, caused by the lack of an overlying gravel

layer, was unknown, and was therefore measured to allow the calculation of sand elevations. A clear acrylic cylinder with a 26.5-cm diameter was filled with gravel from the same population as that in the flume and placed in a manner similar to that in the flume to insure that gravel porosities in the flume and cylinder were approximately equal. Water was added in small volumes to the cylinder, and changes in level of water were measured with a point gauge. The difference between the expected increase in water elevation for the cylinder without gravel and the measured increase in the cylinder with gravel represented the volume of gravel. The porosity was calculated as $P = V_v/V$, where V_v is the volume of the void space, and V is the total volume. The porosity was measured for each water addition, yielding the vertical distribution in Fig. 2. The porosity was relatively constant until the water elevation was approximately 3.0 cm below the maximum gravel elevation.

Table 1. Parameters of the Experiments

Reference number	Discharge designation	Mean discharge (L/s)	Water surface slope	Mean flow depth (m)	Mean flow velocity (m/s)	Bed shear stress (Pa)	Sand position	Froude number	Reynolds number	Particle Reynolds number[a]
1	65	65.7	0.0065	0.224	0.81	11.99	Z_{011}	0.55	181,440	3,836
2	30	30.7	0.0013	0.220	0.39	2.30	Z_{02}	0.27	85,800	1,645
3	50	53.4	0.0038	0.224	0.66	6.99	Z_{02}	0.45	147,840	2,850
4	65	64.6	0.0065	0.220	0.81	12.08	Z_{02}	0.55	178,200	3,742
5	30	30.0	0.0012	0.221	0.38	2.10	Z_{06}	0.26	83,980	1,505
6	50	51.6	0.0037	0.216	0.66	6.57	Z_{06}	0.45	142,560	2,648
7	65	65.8	0.0067	0.220	0.83	12.52	Z_{06}	0.56	182,600	3,657
8	65	65.9	0.0066	0.220	0.83	12.25	Z_{16}	0.56	182,600	3,227
9	50	50.9	0.0036	0.217	0.65	6.09	Z_{32}	0.45	141,050	1,888
10	65	64.5	0.0059	0.217	0.83	10.60	Z_{32}	0.57	180,110	2,421
11	30	26.6	0.0011	0.222	0.33	1.92	Z_{51}	0.22	73,260	756
12	50	51.5	0.0030	0.219	0.65	5.16	Z_{51}	0.44	142,350	1,226
13	65	62.5	0.0056	0.217	0.80	10.18	Z_{51}	0.55	173,600	1,734
14	30	27.2	0.0011	0.214	0.35	1.98	Z_{67}	0.24	74,900	515
15	50	50.4	0.0030	0.214	0.66	5.19	Z_{67}	0.46	141,240	827
16	65	62.6	0.0047	0.208	0.84	7.89	Z_{67}	0.59	174,720	1,023
17	30	27.2	0.0011	0.217	0.35	2.00	Z_{79}	0.24	75,950	338
18	50	49.7	0.0032	0.217	0.64	5.67	Z_{79}	0.44	138,880	550
19	65	62.3	0.0055	0.209	0.83	9.48	Z_{79}	0.58	173,470	735
20	20	20.5	0.0009	0.208	0.27	1.66	Z_{88}	0.19	56,160	81
21	30	28.1	0.0012	0.211	0.37	2.00	Z_{88}	0.26	78,070	202
22	50	51.2	0.0036	0.212	0.67	6.19	Z_{88}	0.46	142,040	356
23	65	61.7	0.0048	0.206	0.83	8.09	Z_{88}	0.58	170,980	407
24	30	27.5	0.0010	0.210	0.36	1.59	Z_{94}	0.25	75,600	104
25	50	48.8	0.0026	0.209	0.65	4.25	Z_{94}	0.45	135,850	165
26	65	62.8	0.0053	0.205	0.85	8.73	Z_{94}	0.60	174,250	236
27	20	20.0	0.0006	0.205	0.27	0.91	Z_{98}	0.19	55,350	31
28	30	27.7	0.0010	0.204	0.38	1.49	Z_{98}	0.27	77,520	40
29	50	48.6	0.0025	0.203	0.66	3.88	Z_{98}	0.47	133,980	64
30	65	62.6	0.0056	0.204	0.85	9.34	Z_{98}	0.60	173,400	99

[a]Grain size of bed calculated as weighted average of sand and gravel exposure from CPDG at the elevation of the mean sand bed.

Experimental Results

Bed Forms

Sand transport was dominated by bed load in the 20, 30, and 50 L/s experiments with Rouse numbers [$Ro = w/(0.4u^*)$; w-fall velocity of sand calculated from Wu and Wang (2006); and $u^* = \sqrt{\tau_b/\rho}$] greater than one (1.2–2.5) in all of these experiments. The 65 L/s experiments had more sand moving as suspended load with Rouse numbers of about 0.9, but also with significant transport of sand as bed load. No streaks or zones of preferred transport were noticed in the experiments because of the sand being transported through the rough bed. In the 20- and 30−L/s experiments, particularly when the sand level was significantly below the top of the gravel, the sand moved in a series of short jumps from sand patch to sand patch. As more sand was added to the channel, the sand tended to preferentially collect in one location. The first unambiguous evidence of regular fluctuations of sand transport was observed in the density cell data when the sand bed was located at Z_{67} (Fig. 5) for the 65−L/s flow. Observing the bed forms directly was difficult because of the long lengths and low heights; however, the bed forms were measured with a time record of the acoustic underwater distance sensor and were found to correspond with changes in sediment concentration (Fig. 6). As the elevation of the sediment bed was increased, regular fluctuations of the total sediment load were also recognized from sediment concentrations measured with the density cell for the experiments with lower flow discharges.
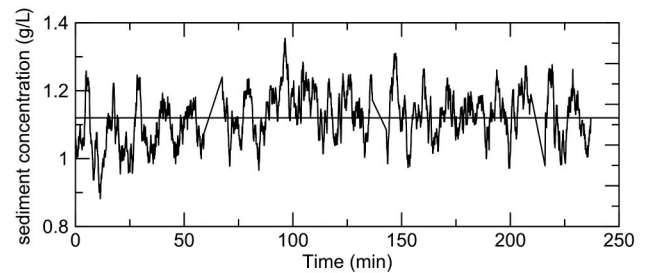

Fig. 5. Sand concentration with time from the density cell for a flow rate of 65 L/s and sand elevation of Z_{67}; data have been filtered using a 15-term moving average

Spacing of the bed forms ranged from one to several meters in length and from several millimeters to 3.5 cm in height. Migration rates of bed forms decreased from 0.006 to 0.004 m/s, and the bed form heights increased from 1.1 to 3.5 cm in the 50−L/s experiments when sand in the bed was at the Z_{79} to Z_{94} levels, whereas migration rates decreased from 0.017 to 0.014 m/s and heights increased from 2.5 to 3.1 cm in the 65−L/s experiments when sand in the bed was at the Z_{88} to Z_{98} levels. The bed shear stress decreased by 35, 44, and 32% for the 30, 50, and 65−L/s experiments, respectively, as sand elevation in the bed increased. The bed roughness decreased as the gravel was progressively buried and the sand began to move in long and low bed forms (Fig. 7), which did not increase the roughness of the boundary,
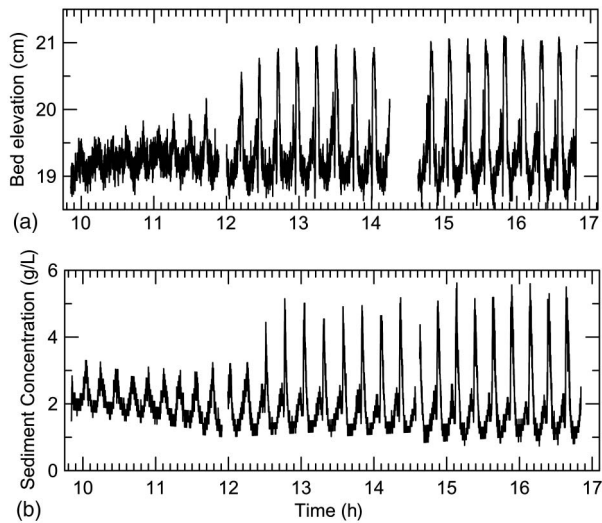
Fig. 6. Bed form development from a flat bed: (a) bed elevation; (b) sediment concentration records collected simultaneously with flow discharge of 65 L/s and sand located at Z_{88}; peaks in sand concentration occurred on average 5.8 min later than the peaks in bed elevation reflecting the 5.51 m the bed form migrated from the bed surface measuring station to the tailbox
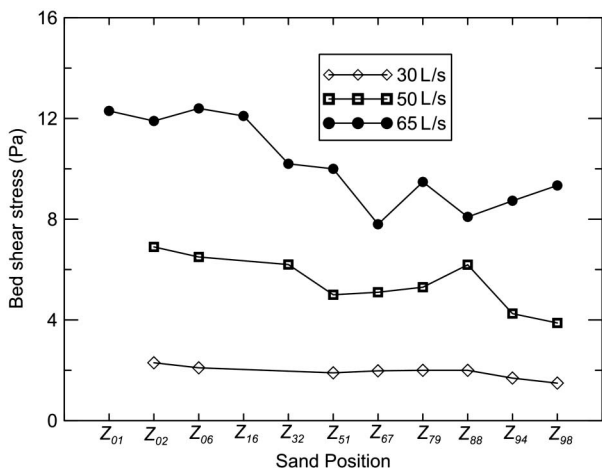

Fig. 7. Bed shear stress with sand elevations for the flow rates of 30, 50, and 65 L/s

as the heights of the bed forms generally did not protrude significantly above the level of the gravel. In the experiments where the elevation of sand was closer to the top of the gravel, the bed forms had a shorter spacing, and multiple forms were present on the flume channel at one time (Fig. 8). Most of the bed forms observed in this study would be classified as small dunes on the basis of their dimensions, the sediment size, and flow strength (Kleinhans 2002; Kuhnle et al. 2006). It is expected that as the sand elevation continued to increase relative to the gravel, the bed forms would transition to dunes typical of sand-bed streams.

Flow Characteristics

Velocity profiles from a companion study (Wren et al. 2011) with the same flume, sediments, and flow conditions as those in the present study will be briefly described next. Only information
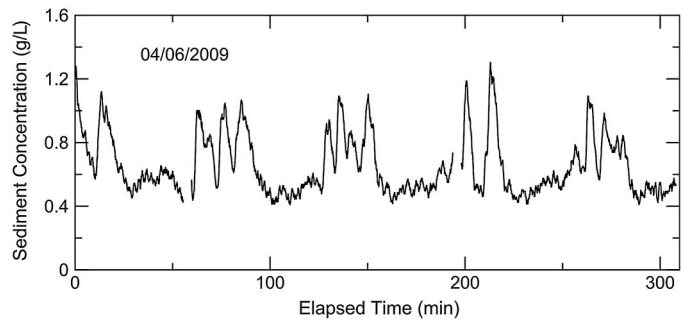
Fig. 8. Sediment transport fluctuations measured by density cell with flow discharge of 50 L/s and sand elevation located at Z_{94}; data have been filtered using a 15-term moving average

considered directly relevant to the present work will be included; for detailed discussions of flow and turbulence, please see Wren et al. (2011). Velocity profiles were collected over a sampling region that was 0.2-m wide and 0.5-m long. Data were first time-averaged for 2 min, and then spatially averaged for six elevations in bed-parallel planes with 42 points per plane. Downstream velocities showed only small changes for different sand levels in the bed (Fig. 6 of Wren et al. 2011), whereas Reynolds stress profiles (Fig. 7 of Wren et al. 2011) displayed decreasing magnitudes throughout the profile as sand elevations in the gravel increased. The Reynolds stress profiles also displayed a typical decreasing trend near the rough bed, as described previously by Raupach et al. (1991) and Nikora et al. (2001). The decrease in Reynolds stress near and below the top of the bed may represent energy extracted by form drag, resulting in a reduction in shear stress applied to sand grains among the gravel particles. Use of the Reynolds stress at the mean elevation of the sand bed was explored as a method of determining the shear stress acting to transport the sand grains. However, the use of the Reynolds stress at the elevation of the sand bed did not improve the relation between sand transport rate and shear stress. To facilitate comparisons with other studies, the sidewall corrected shear stresses were chosen as the appropriate flow strength parameter to represent the mean stress acting on the sand and gravel beds.

Transport of Sand

The relation between bed shear stress and sand transport rate was explored by comparing nondimensional quantities:

$$\tau_{bs}^* = \frac{\tau_b}{(s-1)\rho g D_s} \tag{2a}$$

$$q_s^* = \frac{q_s}{[(s-1)g D_s]^{1/2} \rho_s D_s} \tag{2b}$$

where s = ratio of the density of the sediment (ρ_s) to the density of the water (ρ); D_s = median diameter of the sand; and q_s = transport rate of the sand in mass per time per unit width. It is apparent (Fig. 9) that there is essentially no relation between dimensionless sand transport rate and dimensionless bed shear stress in the experimental runs of this study. As sand elevations in the bed increased relative to the gravel, the transport rates increased by three orders of magnitude while the bed shear stress decreased moderately ($\sim$35%). There is some evidence for negative relations between transport rate and shear stress as seen by the three collections of negatively sloping points that correspond to the experiments with 30, 50, and 65$-$L/s discharges (Fig. 9). The patterns of sand transport rate and bed shear stress (Fig. 9) were attributed to the form
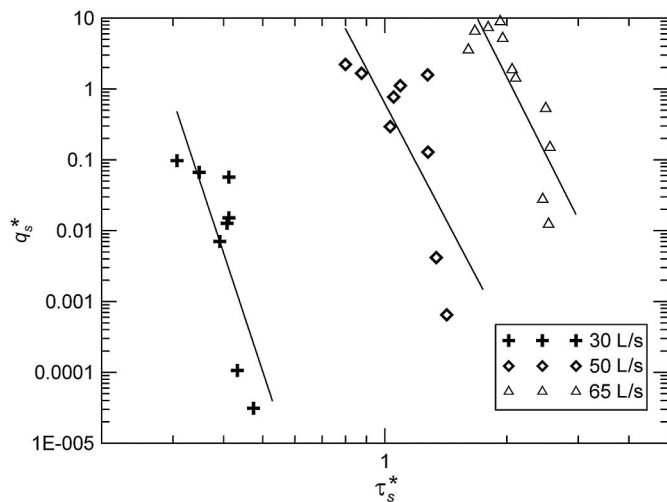
Fig. 9. Dimensionless sediment transport rate versus dimensionless bed shear stress for all 11 beds; the three lines illustrate negative relations between q_s^* and τ_b^* for the experiments with flow rates of 30, 50, and 65 L/s

drag of the gravel, which decreased as the gravel became buried by increasing levels of sand. A successful method to predict the sand transport rate will have to account for a separation of the form drag from the grain stress acting on the sand, along with changes in both amount of shear needed to entrain sand that is submerged in the gravel and the increasing supply of sand as the elevation is increased relative to the gravel.

Comparison to Other Transport Relations Developed for Similar Conditions

Relationships developed to predict sand transport in gravel streams were evaluated to determine their suitability for predicting transport rates in this system. The relation from Wilcock and Kenworthy (2002) was developed as a two-part transport relation for channels with sand and gravel in the bed material. Although the work presented by Tuijnder (2010) and by Grams and Wilcock (2007) is similar to that described presently, neither relation was found to be applicable to the transport conditions of this study. The relation developed by Grams and Wilcock (2007) was formulated to predict the transport of suspended sediment by estimating the rate of entrainment of sand into suspension near the bed and so was not suitable for direct comparison to the bed-load dominated transport data collected in this study. Also near-bed sediment concentration measurements were not collected in this study, preventing the comparison to the relation of Grams and Wilcock (2007). Tuijnder (2010) developed a relationship to predict sand transport as bed load for streams with limited sand and nonmoving fine-to-medium gravel on the bed. However, one of the key variables used by Tuijnder was the average sand layer thickness on top of the immobile layer (d). This variable is necessary to predict bed form dimensions, the fraction of the bed with the immobile layer exposed, and the roughness of the bed. It is problematic to apply the transport relation of Tuijnder to this data because the average elevation of the sand layer was below the top (Z_{100}) of the gravel layer. The relation of Tuijnder therefore predicted no transport of sand for the conditions of this study, most likely attributable to the large differences in the ratio of the gravel to the sand diameters of the two studies (10 versus 100).

Comparison to Transport Relation of Wilcock and Kenworthy (2002)

The transport relation of Wilcock and Kenworthy (2002) (WK) assumes that the sand and gravel fractions of the bed material sediment may be adequately represented by two size groups. It was developed using field and laboratory data, and it has been demonstrated that sand and gravel transport in systems with a near continuous range of sizes in the bed material may be reasonably represented. The main equations of the WK relation are

$$W_i^* = 0.002\phi^{7.5} \quad \text{for } \phi < 1.19 \tag{3a}$$

$$W_i^* = 70\left(1 - \frac{0.908}{\phi^{0.25}}\right)^{4.5} \quad \text{for } \phi \geq 1.19 \tag{3b}$$

where $i = s$ represents the sand fraction and $i = g$ represents the gravel fraction; $\phi = \tau/\tau_{ri}$; τ = bed shear stress; τ_{ri} = reference shear stress of either the sand (τ_{rs}) or gravel fraction (τ_{rg}); $W_i^* = [(s-1)gq_{bi}]/[F_i u_*^3]$; F_i = proportion of sand or gravel in the bed surface; $u_* = \sqrt{\tau/\rho}$ = shear velocity; and q_{bi} = volumetric transport rate per unit width of either sand or gravel. The dimensionless reference shear stress of the sand is defined as

$$\tau_{rs}^* = 0.065 + (4.086 - 0.065)e^{-14F_s} \tag{4}$$

where τ_{rs}^* is rendered dimensionless as in Eq. (2a); and F_S = fraction of sand in the bed surface layer. To calculate sand transport rates for the experiments of this study using the WK relation, the fraction of sand in the bed surface was assumed to be equal to the value of the CPDG (Fig. 2) at the mean elevation of the sand in the bed. The ratio of the predicted to measured sand transport is plotted in Fig. 10. The predicted sand transport rates from the WK relation were much less than the measured ones when the sand elevation was below Z_{16}. For the sand elevations above Z_{16}, predicted rates were about 10 times greater than measured and approached 1 as the sand elevation became near the top of the gravel layer. The low values of the predicted-to-measured ratios in the left part of Fig. 10 likely resulted from the overly large values of the reference shear stress predicted by Eq. (4), whereas the values above the line of perfect agreement may have resulted because
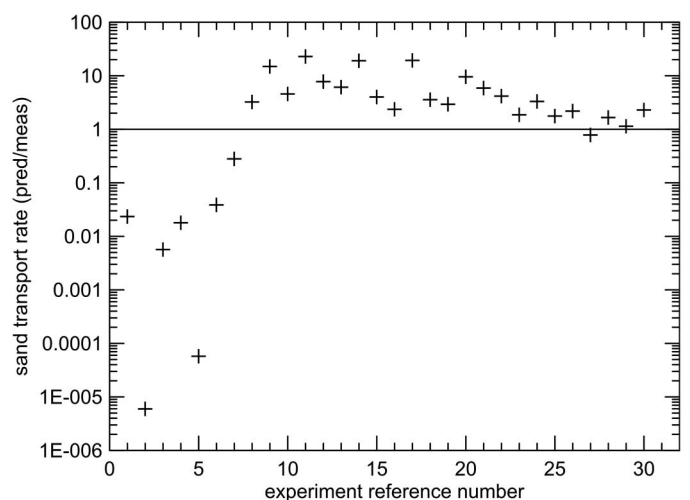

Fig. 10. Comparison between sand transport rates calculated with relation of Wilcock and Kenworthy (2002) and sand transport data measured in this study (for key to experiment reference number see Table 1)

JOURNAL OF HYDRAULIC ENGINEERING © ASCE / FEBRUARY 2013 / **173**

the bed shear stress used in Eq. (3) was larger than that available for transport within the gravel bed because of the sheltering effect of the gravel particles.

Sediment Transport Relation for Sand

The trial applications of the transport relations of Tuijnder and Wilcock and Kenworthy to these data indicated that a different procedure was needed to predict the sand transport rate for the conditions of these experiments. The pattern shown in Fig. 9 suggests that the shear stress available for transporting sand could be decreasing for sand elevations below the top of the gravel. In general, the transport of the sand in this system may be expected to have the following functional relationship:

$$q_s^* = f\left(\frac{\tau_b}{\tau_{cs}}, D_s, \sigma, \mathsf{R}_{pg}\right) \qquad (5)$$

where τ_{cs} = critical shear stress for initiation of motion of the sand of size D_s, which was calculated graphically using the updated Shields-type relation of Miller et al. (1977); σ = standard deviation of the sediment size; and R_{pg} = particle Reynolds number. If the assumption is made that the flow is in the fully rough turbulent stage when sediment is in transport (Table 1), R_{pg} may be dropped and, for moderately well sorted sand size distributions, σ may be assumed to be of secondary importance and is also dropped from consideration. This leaves a transport relation of the form

$$q_s^* = f\left(\frac{\tau_b}{\tau_{cs}}\right) \qquad (6)$$

in which the median size of the sand (D_s) is included in τ_{cs} and q_s^*.

It is apparent from Fig. 9 that there was a poor relation between sand transport rate and total bed shear stress. An initial attempt at drag partitioning to calculate grain shear stress for the sand was made using the procedure of Einstein (1950) as described in Garcia (2008, p. 100). This procedure was not used, however, because calculated grain shear stresses were essentially constant for each flow rate for the range of sand bed elevations. To define a sand transport relation in this system, a method was needed to determine the net shear stress that was acting on the sand below the top of the gravel and represents the increased difficulty of sand entrainment when the sand was submerged in the gravel.

The cumulative probability distribution of the gravel bed surface elevations was used to scale the bed shear stress in the gravel (Fig. 11). The CPDG has several attributes that make it a good choice for this purpose. The CPDG ranges from zero at the lowest elevation of the gravel surface to a value of one at the top of the highest grain on the surface of the bed. The CPDG statistically describes the roughness of the gravel bed. When the CPDG is evaluated at the mean elevation of the sand (z_s) in the gravel bed, it represents the fractional surface exposure of the sand:

$$A(z = z_s) = \frac{A_s(z = z_s)}{A_s(z = z_s) + A_g(z = z_s)} \qquad (7)$$

where A_s and A_g = area of sand and area of gravel, respectively, at the mean elevation of the sand. Following Pellachini (2011), it was the authors' supposition that the shear stress available for transport would be some function of the CPDG evaluated at the mean elevation of the sand:
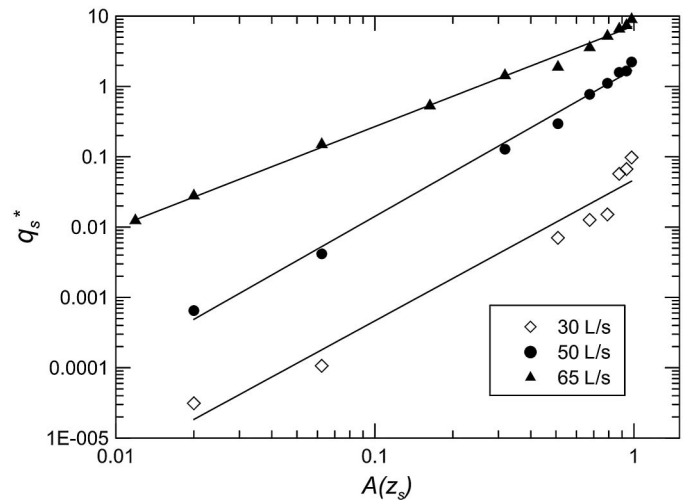
$$\tau_e = f[A(z_s)] \qquad (8)$$

Fig. 11. Relation of dimensionless sand transport rate to $A(z_s)$

where τ_e = shear stress acting on the sand grains within the gravel substrate.

Principal component analysis (PCA) was performed on a data matrix consisting of the sand transport rate, shear stress, and CPDG in log space. The result of this analysis is a new orthogonal coordinate system aligned with the principal axes of variance in the data represented by the eigenvectors of the covariance matrix (Hsieh 2009). The eigenvalue of each vector represents the variance of the data in the direction of the new principal component vector. The proportion of the total variance aligned with each principal component was 0.879, 0.117, and 0.002. Thus, the analysis showed that 99% of the variance in the data could be captured using only two of the three principal components. Because the principal component vectors are linear combinations of q_s, τ, and $A(z_s)$, this provided a relation between the variables that minimizes the resulting variance. That is, most of the variance in the sand transport rate could be accounted for using only the CPDG and shear stress as explanatory variables. The new relation for the data, which represents a best fit, is given as

$$q_s^* = 2.29 \times 10^{-5} [A(z_s)]^{2.14} \left(\frac{\tau_b}{\tau_{cs}}\right)^{3.49} \qquad (9)$$

with a coefficient of determination, r-squared, equal to 0.94 (Fig. 12).

Discussion

The prediction of the transport rate of sand in a nonmobile gravel bed is a difficult problem that this study has made headway towards solving. The main finding, that the shear stress affecting the sand in the gravel bed decreases with depth below the top of the gravel and may be predicted as a function of the CPDG, appears reasonable and is based on the physical distribution of the material in the top layer of the sediment bed. In addition to affecting the shear stress, the correction term may also be interpreted to include the effect of the reduced area of sand exposed to the flow and the increased shear stress necessary to entrain sand grains buried in the gravel, as the mean sand elevation becomes farther below the top of the gravel layer. Application of this technique requires information on the CPDG of the gravel bed and the average height of the sand relative to the gravel. The distribution of heights associated with the gravel bed and the location of the sand within it would need to be
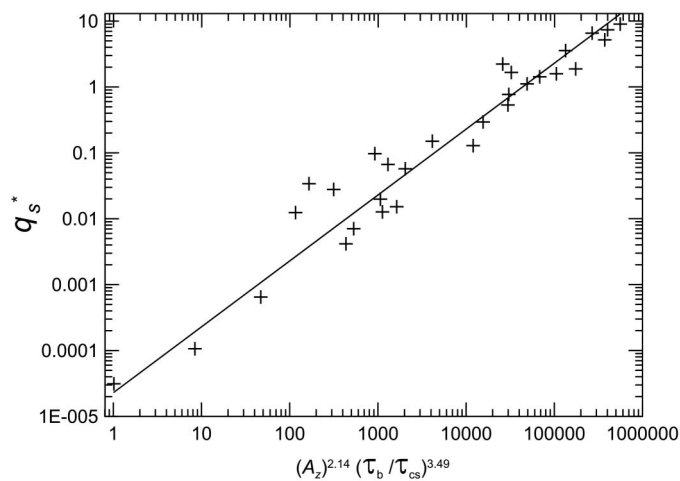
Fig. 12. Dimensionless transport rate versus effective shear stress; equation of best-fit line is $q_s^* = 2.29 \times 10^{-5}[A(z_s)]^{2.14}(\tau_b/\tau_{cs})^{3.49}$, with $r^2 = 0.94$

measured directly over a representative area and combined with measured flow data to apply this technique. Recent work by Stoesser (2010) shows promise to allow the prediction of the CPDG from information on the grain size of bed material.

The use of a correction function to represent the shear stress acting on the sand is similar to but different than the findings from the related study of Grams and Wilcock (2007) (GW). In the GW study, a correction function related to the sand elevation in a bed of 10-cm hemispheres was developed for the sand entrainment rate near the bed. The correction function had the form of a fitted logistic function that ranged from zero to one as the normalized sand elevation on the bed also varied from zero to one. It was observed by GW that the correction function went to unity when the normalized sand elevation (ratio of sand cover thickness to characteristic roughness height of coarse grains) was approximately 0.5, which implied an enhanced rate of entrainment indistinguishable from a 100% sand bed when the normalized sand elevation was greater than 0.5. In this study, a correction term, based on the elevation of the sand in the bed relative to that of the gravel, was also defined, but it was determined from the measured cumulative distribution of elevations of the gravel bed. The value of the correction function in this study does not approach unity until the normalized sand elevation is approximately 0.9. It is possible that the correction functions in this study were different than in the GW study because the majority of the sand in the GW study was transported in suspension, whereas in this study the majority of the sand was transported as bed load.

One concern with this methodology to predict sand transport in coarser gravel is its generality. At the time of writing this manuscript, experiments of sand transport over cobbles with a median size of 150 mm are in progress. Preliminary analysis of results indicates that the same methodology used here successfully predicts sand transport in this much coarser system. For both the gravel and cobble substrates, the procedure yields reasonably accurate predictions. Further work will be needed to determine whether this technique will be directly applicable to field streams; however, the similar behavior of these two systems allows the authors to be cautiously optimistic regarding the potential for application in streams with different sediment and flow conditions.

The current set of experiments indicates that sand transport among the gravel was related to the mean sand depth relative to the gravel geometry and the shear stress to the power of 3.5

[Eq. (9)]. It is reasonable to assume that Eq. (9) will transition as the gravel bed is gradually buried to follow a relation for pure sand beds, with the exponent of shear stress at a lower value (1.5–2.5; Vanoni 1975; Garcia 2008). As the sand elevation in the gravel bed increases, the fraction of the bed shear stress on the sand increases, the area of the sand exposed to the flow increases, the shielding effect of the gravel on the sand diminishes, and thus the exponent on shear stress greater than for a pure sand bed results [Eq. (9)]. When the gravel is completely covered by the sand, increases in bed shear stress will only affect the flow strength available for sand transport, and the rate of growth in transport rate for a given shear strength increase would be expected to be less than in the experiments in this study. The exact nature of the transition between the transport relation identified in this study [Eq. (9)] and one for pure sand is a matter for further research.

Conclusions

Experiments in a laboratory flume channel have indicated that the elevation of the sand in a nonmoving gravel bed was a key variable controlling its transport rate. As the mean elevation of the sand was increased relative to the gravel, transport of the sand was observed to increase by about three orders of magnitude while the bed shear stress gradually decreased. The decrease of the bed shear stress was attributed to the decreasing roughness of the bed surface as the gravel bed became buried by the sand.

Bed forms were observed in the flume channel when the sand elevation was at Z_{67} or greater and became very regular in spacing and migration rate when the sand bed reached the Z_{79} level. The spacing of the bed forms was on the order of meters and heights of several millimeters to about 3.5 cm. The bed forms became less constant in spacing and migration rate as the sand elevation and transport rate increased. Bed forms observed in this study had a minor effect on the bed shear stress.

The sand transport data in this study were compared with predicted values from published transport relations developed for similar systems, but the predictions generally corresponded poorly with measured rates. The lack of correspondence between predicted and measured data was attributed to difficulties in estimating the applied shear stress on the sand fraction. It was found that the bed shear stress scaled by the square of the cumulative probability distribution of the gravel evaluated at the mean elevation of the sand provided a reasonable correlation between sand transport rate and shear stress. Likely, the CPDG evaluated at the elevation of the sand functioned to correct for changes in the area and entrainability of the sand and the fraction of shear stress available for sand transport with depth in the gravel layer. This information will be useful for determining the fate of sand introduced to channels downstream of dams and will improve efforts to manage streams of this type. Comparison with data collected under a wider range of both coarse and fine sediment sizes is needed to establish the generality of this work.

References

Aberle, J., Koll, K., and Dittrich, A. (2008). "Form induced stresses over rough gravel-beds." *Acta Geophys.*, 56(3), 584–600.

Almedeij, J. H., Diplas, P., and Al-Ruwaih, F. (2006). "Approach to separate sand from gravel for bed-load transport calculations in streams with bimodal sediment." *J. Hydraul. Eng.*, 132(11), 1176–1185.

Alonso, C. V., Theurer, F. D., and Zachmann, D. W. (1996). "Sediment intrusion and dissolved-oxygen transport model—SIDO." Technical Rep. *No. 5*, USDA-ARS National Sedimentation Laboratory, Oxford, MS.

Bouguet, J.-Y. (2008). "Camera calibration toolbox for Matlab®."⟨http://www.vision.caltech.edu/bouguetj/calib_doc/index.html⟩ (Jul. 2, 2008).

Manes, C., Pokrajac, D., and McEwan, I. (2007). "Double-averaged open-channel flows with small relative submergence." *J. Hydraul. Eng.*, 133(8), 896–904.

Chiew, Y. M., and Parker, G. (1994). "Incipient motion on non-horizontal slopes." *J. Hydraul. Res.*, 32(5), 649–660.

Cooper, J. R., and Tait, S. J. (2008). "The spatial organization of time-averaged streamwise velocity and it correlation with the surface topography of water-worked gravel beds." *Acta Geophys.*, 56(3), 614–641.

Curran, J. C., and Wilcock, P. R. (2005). "Effect of sand supply on transport rates in a gravel-bed channel." *J. Hydraul. Eng.*, 131(11), 961–967.

Einstein, H. A. (1950). "The bed load function for sediment transportation in open channel flows." *Technical Bulletin 1026*, Soil Conservation Service, U.S. Dept. of Agriculture, Washington, DC.

Ferguson, R. I., Prestegaard, K. L., and Ashworth;, P. J. (1989). "Influence of sand on hydraulics and gravel transport in a braided gravel bed river." *Water Resour. Res.*, 25(4), 633–643.

Garcia, M. H. (2008). "Sediment transport and morphodynamics." Chapter 2, *Sedimentation engineering, processes, measurements, modeling, and practice*, M. H. Garcia, ed., American Society of Civil Engineering, Reston, VA, 21–163.

Gibson, S., Abraham, D., Heath, R., and Schoellhamer, D. (2009). "Vertical gradational variability of fines deposited in a gravel framework." *Sedimentology*, 56(3), 661–676.

Grams, P. E., and Wilcock, P. R. (2007). "Equilibrium entrainment of fine sediment from a coarse immobile bed." *Water Resour. Res.*, 43(10), W10420.

Hardy, R. J., Best, J. L., Land, S. N., and Carbonneau, P. E. (2009). "Coherent flow structures in a depth-limited flow over a gravel surface: The role of near-bed turbulence and influence of Reynolds number." *J. Geophys. Res.*, 114, F01003.

Hathaway, G. A. (1948). "Observations on channel changes, degradation, and scour below dams." *Research Project No. 2*, Appendix 16, International Association on Hydraulic Structures, Stockholm, Sweden, 287–307.

Horton, J. K. (2001). "Flow and bedform dynamics of a bimodal sand-gravel mixture." Ph.D. thesis, School of Earth Science, Univ. of Leeds, Leeds, UK.

Hsieh, W. W. (2009). *Machine learning methods in the environmental sciences: Neural networks and kernels*, Cambridge Univ. Press, Cambridge, UK.

Iseya, F., and Ikeda, H. (1987). "Pulsations in bedload transport rates induced by a longitudinal sediment sorting: A flume study using sand and gravel mixtures." *Geografiska Annaler*, 69A(1), 15–27.

Kleinhans, M. G. (2002). "Sorting out sand and gravel: Sediment transport and deposition in sand-gravel bed rivers." *NGS 293*, Netherlands Geographical Studies, Utrecht University, Utrecht, Netherlands.

Kuhnle, R. A. (1992). "Fractional transport rates of bed load on goodwin creek." *Dynamics of gravel bed rivers*, P. Billi, R. D. Hey, C. R. Thorne, and P. Tacconi, eds., Wiley, Chichester, UK, 141–155.

Kuhnle, R. A. (1993). "Fluvial transport of sand and gravel mixtures with bimodal size distributions." *Sediment. Geol.*, 85(1–4), 17–24.

Kuhnle, R. A., Horton, J. K., Bennett, S. J., and Best, J. L. (2006). "Bed forms in bimodal sand-gravel sediments: Laboratory and field analysis." *Sedimentology*, 53(3), 631–654.

Lane, S. N., James, T. D., and Crowell, M. D. (2000). "Application of digital photogrammetry to complex topography for geomorphological research." *Photogramm. Rec.*, 16(95), 793–821.

Leica Geosystems. (2002). *IMAGINE OrthoBASE user's guide*, GIS and Mapping Division, Atlanta.

Lisle, T. E., and Lewis, J. (1992). "Effects of sediment transport on survival of salmonid embryos in a natural stream: A simulation approach." *Can. J. Fish. Aquat. Sci.*, 49(11), 2337–2344.

McLean, S. R., and Nikora, V. I. (2006). "Characteristics of turbulent unidirectional flow over rough beds: Double-averaging perspective with particular focus on sand dunes and gravel beds." *Water Resour. Res.*, 42(10), W10409.

Mignot, E., Barthelemy, E., and Hurther, D. (2009). "Double-averaging analysis and local flow characterization of near-bed turbulence in gravel-bed channel flows." *J. Fluid Mech.*, 618(1), 279–303.

Miller, M. C., McCave, I. N., and Komar, P. D. (1977). "Threshold of sediment motion under unidirectional currents." *Sedimentology*, 24(4), 507–527.

Nikora, V., Goring, D., McEwan, I., and Griffiths, G. (2001). "Spatially averaged open-channel flow over rough bed." *J. Hydraul. Eng.*, 127(2), 123–133.

Nikora, V., McEwan, I., McLean, S., Coleman, S., Pokrajec, D., and Walters, R. (2007a). "Double-averaging concept for rough-bed open-channel and over-land flows: Theoretical background." *J. Hydraul. Eng.*, 133(8), 873–883.

Nikora, V., et al. (2007b). "Double-averaging concept for rough-bed open-channel and over-land flows: Applications." *J. Hydraul. Eng.*, 133(8), 884–895.

Papanicolaou, A. N., Dermisis, D. C., and Elhakeem, M. (2011). "Investigating the role of clasts on the movement of sand in gravel bed rivers." *J. Hydraul. Eng.*, 137(9), 871–883.

Parker, G. (2008). "Transport of gravel and sediment mixtures." Chapter 3, *Sedimentation engineering, processes, measurements, modeling, and practice*, M. H. Garcia, ed., American Society of Civil Engineering, Reston, VA, 165–251.

Parker, G., Klingemen, P. C., and McLean, P. G. (1982). "Bedload and size distribution in paved gravel-bed streams." *J. Hydraul. Div.*, 108(4), 544–571.

Pellachini, C. (2011). "Modelling fine sediment transport over an immobile gravel bed." Ph.D. thesis, Univ. of Trento, Trento, Italy.

Raupach, M. R., Antonia, R. A., and Rajagopalan, S. (1991). Rough-wall turbulent boundary layers." *Appl. Mech. Rev.*, 44(1), 1–25.

Sambrook Smith, G. H. (1996). "Bimodal fluvial bed sediments: Origin, spatial extent and processes." *Prog. Phys. Geog.*, 20(4), 402–417.

Stoesser, T. (2010). "A physically realistic roughness closure scheme to simulate turbulent channel flow over rough beds within the framework of LES." *J. Hydraul. Eng.*, 136(10), 812–819.

Topping, D. J., Rubin, D. M., and Vierra, L. E. Jr. (2000). "Colorado River sediment transport 1. Natural sediment supply limitation and the influence of Glen Canyon Dam." *Water Resour. Res.*, 36(2), 515–542.

Tuijnder, A. P. (2010). "Sand in short supply, modelling of bedforms, roughness, and sediment transport in rivers under supply-limited conditions." Ph.D. thesis, Univ. of Twente, Enschede, Netherlands.

Vanoni, V. A. (1975). "Sedimentation engineering." *ASCE manuals and reports on engineering practice—No. 54*, American Society of Civil Engineers, Reston, VA.

Vanoni, V. A., and Brooks, N. H. (1957). "Laboratory studies of the roughness and suspended load of alluvial streams." *M.R.D. sediment series, No.11*, California Institute of Technology Sedimentation Laboratory, U.S. Army Engineers Division, Pasadena, CA.

Wilcock, P. R., and Crowe, J. C. (2003). "A surface-based transport model for sand and gravel." *J. Hydraul. Eng.*, 129(2), 120–128.

Wilcock, P. R., and Kenworthy, S. T. (2002). "A two-fraction model for the transport of sand/gravel mixtures." *Water Resour. Res.*, 38(10), 12-1–12-12.

Wren, D. G., Langendoen, E. J., and Kuhnle, R. A. (2011). "Effect of sand addition on turbulent flow over an immobile gravel bed." *J. Geophys. Res.*, 116, F01018.

Wu, W., and Wang, S. S. Y. (2006). "Formulas for sediment porosity and settling velocity." *J. Hydraul. Eng.*, 132(8), 858–862.